

Evolution of electrical resistivity and electronic structure of transuranium metals under pressure: Numerical investigations

Yu. Yu. Tsiovkin,^{1,*} A. V. Lukoyanov,^{1,2} A. O. Shorikov,^{1,2} A. A. Povzner,¹ L. Yu. Tsiovkina,¹ A. A. Dyachenko,¹ V. B. Bystrushkin,¹ M. V. Raybukhina,¹ M. A. Korotin,² V. V. Dremov,³ and V. I. Anisimov²

¹*Ural Federal University, 620002 Yekaterinburg, Russia*

²*Institute of Metal Physics, Russian Academy of Sciences–Ural Division, 620990 Yekaterinburg, Russia*

³*Russian Federal Nuclear Center, Institute of Technical Physics, Snezhinsk, 456770 Chelyabinsk Region, Russia*

(Dated: September 29, 2018)

The influence of electronic structure evolution upon pressure on the temperature dependencies of electrical resistivity of pure Np, Pu, Am, and Cm metals have been investigated within coherent potential approximation (CPA) for many-bands conductivity model. Electronic structure of pure actinide metals was calculated within the local density approximation with the Hubbard U and spin-orbit coupling corrections (LDA+ U +SO) method in various phases at normal conditions and under pressure. They were compared with the corresponding cubic (bcc or fcc) phases. The densities of states of the latter were used as a starting point of model investigations of electrical resistivity. The obtained results were found in good agreement with available experimental data. The nature of large magnitude of resistivity of actinides was discussed in terms of the proposed conductivity model using the *ab initio* calculated parameters.

PACS numbers: 71.27.+a, 71.10.-d, 71.20.-b

I. INTRODUCTION

For many decades transuranium metals have been of interest to scientific community due to the unique combination of structural, electronic, and kinetic properties.¹ Their rich phase diagrams² include a number of structural transitions upon pressure or increasing the temperature.^{3–7} Intermediate or *jj* coupling schemes, in contrast to usual Russel-Saunders (*LS*) one, were found to be more appropriate for $5f$ electrons in transuranium metals due to the presence of large spin-orbit coupling in actinides.^{8–10} Additionally, magnetic stabilization of phases was found in curium.^{5,11} Drastic changes of crystal and electronic structures and their interplay¹² do not deplete this list of unusual properties of the metals.

Anomalous resistance properties in transuranium metals are also well known.¹³ The negative temperature coefficient of resistivity (TCR) was measured in α - and δ -Pu and some Pu-based alloys at high temperatures ($T > \theta_D$).^{14,15} Moreover, $\rho \sim T^2$ dependence was found in these compounds at low temperature.^{13,16,17} Electrical resistivity (ER) behavior in pure Np and Am metals is ordinary,^{18–20} namely, $\rho \sim T$ in high and $\rho \sim T^3$ and $\rho \sim T^{4-5}$ in low temperature ranges, respectively.²¹ The superconducting state was found in Am at ambient pressure with the characteristic temperature $T_c \sim 0.5 - 2.0$ K.²² Curium metal also demonstrates ordinary behavior of ER typical for antiferromagnetic metal with $\rho \sim T^2$ at low temperature and $\rho \sim T$ at high temperature, respectively. However, temperature dependencies of ER in transuranium metals show anomalously high values of ER (typically, $80 \div 140 \mu\text{k}\Omega \cdot \text{cm}$) at room temperature. For comparison, ER of transition metals at the same conditions are about $1 \div 10 \mu\text{k}\Omega \cdot \text{cm}$.

Such high resistivity values of transuranium metals have

no reasonable explanation yet and all previous model investigations substantially underestimate the experimental values of ER. For example, Mott two-band conductivity model combined with coherent potential approximation (CPA) shows, that Np, Pu, Am, and Cm are typical metals at high temperatures,²³ and observed ER behavior is described well in relative units. However, absolute values of ER in transuranium metals cannot be estimated from these calculations. Indeed, the estimation of maximum value of ER – taking into account only interband transitions of scattering conductivity electrons with additional accounting that probabilities are proportional to the DOSes values at the Fermi level – gives the ER values at most $20 \div 40 \mu\text{k}\Omega \cdot \text{cm}$ that underestimates the experimental data by a factor of 3.

It is well known, that the high-resistivity values can be provided by specific Kondo-like resonance. Actinides, usually considered as heavy-fermion systems,¹⁰ should demonstrate appropriate kinetic and magnetic properties in low temperature range. However, we have no experimental data for the detailed discussion in terms of such a model. Previously reported investigations of ER within common Kondo model^{24,25} have a number of problems and ambiguities²⁶ due to selecting of the “magnetic” part of ER. A principal problem arose if one uses spin-fluctuation model²⁷ for describing ER of δ -Pu and other actinides. Indeed, one can find good agreement of calculated and experimental data only adjusting the Stoner factor.¹⁶ However, such a high magnitude of the Stoner factor should result in specific temperature behavior of magnetic susceptibility, typical for amplified paramagnets. In contrast to these expectations, ordinary for paramagnets temperature dependence of magnetic susceptibility was measured in the systems under consideration.²⁴

On the other hand, recent NMR experiments for δ -

Pu revealed a combination of Curie-Weiss and van-Fleck temperature behavior of spin susceptibility.^{28,29} That demonstrates strong influence of spin-density fluctuations on electronic structure and can provide anomalies of electron heat capacity in the same temperature range, as reported in Ref. 30. Actually, strong spin-density fluctuations effects can play a noticeable role in actinides, providing $\rho \sim T^2$ in very low temperature region, and suppressing superconductivity. Note also, that the $\rho \sim T^2$ dependence and negative TCR (observed in δ -Pu) can be described in terms of strong electron-phonon coupling.^{23,31} Thus, theoretical explanation of the high values of resistivity of transuranium metals will require significant efforts, and hence *ab-initio* calculations are of high interest for the understanding of ground state properties in these materials.

Recent experiments and electronic structure calculations revealed numerous effects due to strong correlations of the $5f$ electrons in Np, Pu, Am, and Cm.¹⁰ A number of band methods and approximations have been applied to describe magnetic and spectral properties of transuranium metals.¹⁰ Nonmagnetic ground state of pure plutonium metal observed experimentally³² was reproduced in the electronic structure calculations by the LDA+ U +SO method.³³ There the exchange interaction was found to be the reason of artificial antiferromagnetic ordering in previous LSDA+ U investigations. Also nonmagnetic ground state was obtained in around-mean-field version of the LDA+ U method,³⁴ then in LDA + Hubbard I approximation,^{35,36} and hybrid density functionals with a dominant contribution of HF functional.³⁷ Recently, the reliability of these results was proved by the more detailed analysis of exchange interaction,^{38,39} and also by the LDA+DMFT method,⁴⁰ combining the LDA approximation with the Dynamical Mean-Field Theory (DMFT) in various modifications.^{41–47} However, consistent interpretation of spectroscopic data by these calcu-

lations is not found yet.⁴⁸

In this paper we report the results of electronic structure and resistivity calculations for transuranium metals at normal conditions and under pressure. In terms of CPA the many-band conductivity model was derived and applied for fcc-Pu, Am, and Cm and bcc-Np numerical investigations of electrical resistivity using DOSes of metals calculated within the LDA+ U +SO method as a starting point. The derived model allows one to account for initial DOSes modifications in a direct way as a result of temperature erosion and its renormalization due to interband $s \rightarrow d$, $s \rightarrow f$, $d \rightarrow f$, and $f \rightarrow d$ electron transitions. The DOSes evolution of the metals with temperature at normal conditions and under pressure were presented and discussed. Results of the ER calculations are found in good agreement with available experimental data. In terms of the proposed conductivity model, using *ab initio* obtained parameters, the nature of high-resistivity values in actinides is also discussed.

II. ELECTRONIC STRUCTURE CALCULATIONS

We investigated the electronic structure of transuranium metals within the LDA+ U +SO method described in detail in Ref. 33. In this method the exchange interaction (spin polarization) term in the Hamiltonian is implemented in the general nondiagonal matrix form regarding the spin variables. This form is necessary for correct description of $5f$ electrons for the case of jj and intermediate couplings.³³ The LDA+ U +SO method is introduced by the effective single-particle Hamiltonian which supplements initial local density approximation (LDA) functional by a term with orbital dependent potential $V_{mm'}^{ss'}$, which accounts for Coulomb interactions,⁴⁹ and spin-orbit coupling term:³³

$$\hat{H}_{LDA+U+SO} = \hat{H}_{LDA} + \sum_{ms,m's'} |inlms\rangle V_{mm'}^{ss'} \langle inlm's'| + \lambda \cdot \hat{\mathbf{L}} \cdot \hat{\mathbf{S}}, \quad (1)$$

$$V_{mm'}^{ss'} = \delta_{ss'} \sum_{m'',m'''} \{ \langle m, m'' | V_{ee} | m', m''' \rangle n_{m''m'''}^{-s-s} + (\langle m, m'' | V_{ee} | m', m''' \rangle - \langle m, m'' | V_{ee} | m''', m' \rangle) n_{m''m'''}^{ss} \} \\ - (1 - \delta_{ss'}) \sum_{m'',m'''} \langle m, m'' | V_{ee} | m''', m' \rangle n_{m''m'''}^{s's} - U(N - \frac{1}{2}) + \frac{1}{2} J_H(N - 1). \quad (2)$$

Here U and J_H are screened Coulomb and Hund exchange parameters which are determined in the constrain LDA calculations.^{50,51} The screened Coulomb interaction matrix elements $\langle m, m'' | V_{ee} | m', m''' \rangle$ could be expressed via these parameters.⁴⁹ In the constrain LDA procedure a *screened* Coulomb interaction of $5f$ electrons is evaluated that requires the choice of screening chan-

nels taken into account in the constrain LDA calculations. Taking s , p , and d channels, for Np, Pu, Am, and Cm we obtained the Coulomb parameter value $U \approx 4$ eV in good agreement with the previously used value.⁴¹

In contrast to the direct Coulomb parameter U , the exchange parameter J_H is evaluated as a *difference* of interaction energy for the electrons pairs with the opposite

and the same spin directions. Here the screening process is defined by the charge but not spin state of the ion, then the screening contribution is canceled for exchange Coulomb interaction and parameter J_H does not depend on the choice of screening channels. For neptunium and plutonium, the value of Hund exchange parameter J_H was reported to be $J_H = 0.48$ eV,³³ for americium – 0.49 eV, and for curium – 0.52 eV.^{23,52}

In Eq. (2) the off-diagonal exchange interaction terms with $n_{m''m'''}^{s's'}$ are significant for actinide elements. It was demonstrated in Ref. 33, that omission of these terms can result in incorrect antiferromagnetic ground state for fcc-plutonium metal. This fact is due to the intermediate or jj coupling scheme taking place in most actinide metals, including Pu, Np, and Cm. But in pure Am metal jj coupling is present. It means that total moment \mathbf{J} is well defined, but not spin \mathbf{S} and orbital \mathbf{L} moments, as in usual LS coupling scheme. In this case, the basis of eigenfunctions of total moment operator $\{jm_j\}$ is the best choice. The matrix of spin-orbit coupling operator is diagonal in this basis but not the exchange interaction (spin-polarization) term in the Hamiltonian.

Whereas in the LS coupling scheme \mathbf{S} and \mathbf{L} operators are well defined. Then the basis of LS orbitals, which are eigenfunctions of both spin \mathbf{S} and orbital moment \mathbf{L} operators, is a good choice. In this case it is possible to define quantization axis in the direction of spin moment vector so that occupation and potential matrices will be diagonal in spin variables.

When the intermediate coupling is realized, neither jj basis, nor LS is valid, and occupation matrix is nondiagonal in both orbital bases and both terms in the Hamiltonian: spin-orbit coupling and exchange interaction, must be taken in a general nondiagonal matrix form, and some finer treatment is necessary. Intermediate basis is still cumbersome and is used for model atomic calculations.

For the actinide metals under consideration the LDA+ U +SO densities of states (DOS) were taken as a starting point for further CPA simulations of ER temperature dependencies within the model described below.

III. COHERENT POTENTIAL APPROXIMATION FOR MANY BAND CONDUCTIVITY MODEL

In the general case, the *many-band* conductivity model is suitable for explanation of kinetic properties in actinides due to equal probabilities of transitions of $(s+p)$ electrons into almost empty d and f bands, since the values of DOSes at the Fermi level in d and f bands are close to each other. Thus, ratios between partial d and f DOSes at the Fermi level lead to opening of additional channel of direct $d \rightarrow f$ and back $f \rightarrow d$ electrons transition. Moreover, the evolution of the d and f DOSes with temperature and direct and back transitions depends on the evolution of DOSes of the other shell. Then it is reasonable to obtain DOSes at finite temperatures with

regular self-consistent procedure and derive corresponding CPA set of equations without model simplification, in the same way as it was made previously in Ref. 31, when only direct $s \rightarrow d$ and $s \rightarrow f$ transitions were accounted for.

We start considering the $s(p)$, d , and f electrons performing intra- and inter-band transitions as a result of their scattering at long wave phonons. We assume also that the accepting d or f bands are partially filled. Then the Hamiltonian of electron subsystem $\hat{H} = \hat{H}_0 + \hat{H}_{int}$ can be written down in the following form:

$$\hat{H} = \sum_l E_l \hat{a}_l^+ \hat{a}_l + \frac{1}{N} \sum_{n,l,l'} e^{-i(\vec{k}-\vec{k}',\vec{R}_n)} \hat{V}_{ll'}(n) \hat{a}_l^+ \hat{a}_{l'}, \quad (3)$$

where E_l is a periodical part of electrons energy. Combined index l includes the band index j ($j = s, d, f$) and wave vector \vec{k} ; \vec{R}_n is a radius-vector of the n -th site of a crystal lattice. Operator $\hat{V}_{l,l'}(n)$ describes the intensity of electron-phonon interaction. If thermal displacements of ions are small, the operator $\hat{V}_{l,l'}(n)$ can be written as

$$\hat{V}_{\alpha,l,l'}(n) = Z_{ll'} \frac{-i}{\sqrt{N}} \sum_{\vec{q}} \sqrt{\frac{q_0}{q}} \left[e^{i(\vec{q}\vec{R}_n)} \hat{b}_{\vec{q}} - e^{-i(\vec{q}\vec{R}_n)} \hat{b}_{\vec{q}}^+ \right], \quad (4)$$

where

$$Z_{ll'} = \left(\frac{\hbar K_F}{2MS} \right)^{1/2} \cdot \left(\frac{2K_F}{3q_0} \right)^{1/2} \cdot \Lambda_{l,l'} \quad (5)$$

is the parameter of intensity of intra- and inter-band transitions due to electron-phonon scattering. M and S are the mass and the sound velocity in metal, respectively; q_0 is the maximum value of q and K_F is the Fermi wave number of electron; $\Lambda_{l,l'}$ are the (Bloch) parameters of electron-phonon coupling.

Using *ab-initio* obtained DOSes of metal as a starting point of numerical calculations we assume that effects of s , p , d , f hybridization are accounted for in the electron ground state. For simplicity we keep the same band notations after renormalization.

A set of CPA equations can easily be derived using Dyson equation and definition of T-matrix. Let us determine the total resolvent of the full energy operator \hat{H} :

$$\hat{R} = (z - \hat{H})^{-1}, \quad (6)$$

and the strictly diagonal part of the total resolvent \hat{R} in the \hat{H}_0 representation:

$$\hat{G} = (z - \hat{H}_0 - \hat{\Delta})^{-1}, \quad (7)$$

where $\hat{\Delta}$ is a strictly diagonal shift operator in the \hat{H}_0 representation. Broadening of single electron levels is described as:

$$\hat{\Delta} = \frac{1}{N} \sum_{n,l,l'} e^{-i(\vec{k}-\vec{k}',\vec{R}_n)} \Delta_j \delta_{jj'} \hat{a}_l^+ \hat{a}_l. \quad (8)$$

The real part of the coherent potential Δ_j determines the shift η_j , and its imaginary part γ_j determines the broadening of single-electron levels.

To derive equations within many-band CPA, the Dyson identity was used:

$$\hat{R} = \hat{G} + \hat{G}(\hat{V} - \hat{\Delta})\hat{R}. \quad (9)$$

Scattering operator \hat{T} can be determined in a convenient form as:

$$\hat{R} - \hat{G} = \hat{G}\hat{T}\hat{G}. \quad (10)$$

Multiplying both parts of identity (10) by \hat{G}^{-1} , one obtains the following expression for the scattering operator:

$$\hat{T} = \hat{G}^{-1}(\hat{R} - \hat{G})\hat{G}^{-1}. \quad (11)$$

Using the Dyson identity (9) and Eq. (11) for the shift operator, the following operator series can be written:

$$\hat{\Delta} = [(\hat{V} - \hat{\Delta})\hat{G}(\hat{V} - \hat{\Delta}) + (\hat{V} - \hat{\Delta})\hat{G}(\hat{V} - \hat{\Delta})\hat{G}(\hat{V} - \hat{\Delta}) + \dots]_{diag}. \quad (12)$$

Here the *diag* index means that the diagonal part in the \hat{H}_0 representation of the sum of operator products in

brackets should be taken. The series (12) contains mutually compensated block terms, in which the shift operator is included in indirect form.⁵³ Excluding the compensated block terms from Eq. (12), and averaging over ion displacements, one finally obtains the shift operator as

$$\langle \hat{\Delta} \rangle = \left\langle \left[\hat{V}\hat{G}\hat{V} + \hat{V}\hat{G}\hat{V}\hat{G}\hat{V} + \dots \right]_D \right\rangle. \quad (13)$$

Here only strictly diagonal terms in the \hat{H}_0 representation ($[...]_D$) are accounted for, and items containing the blocks are omitted. The brackets $\langle \dots \rangle$ mean averaging over phonons. Let us assume also, that at high temperature the operator $\hat{V}_{ll'}(u)$ can be replaced with the one averaged over wave vectors \vec{k} and \vec{k}' functions of fluctuating variable $u - V_{n,jj'}(u)$.⁵⁴ Then the series (13) can be summed up accurately (in the convergence range $|V_j(u)F_j| < 1$) as it is shown in the Appendix for single-electron and single-site approaches. Using for simplification also $|V_{n,sj}(u)F_s| \ll 1$, $|V_{n,s}F_s| / |V_{n,(d)f}F_{(d)f}| \ll 1$, $|V_{sj}F_s| / |V_{jj'}F_j| \ll 1$ and notation $V_{n,jj}(u) = V_{n,j}(u)$, for the averaging over ion thermal displacements s - and d -band coherent potentials, one obtains:

$$\Delta_s = \sum_{j \neq j'} \int_{-\infty}^{\infty} du P(u) \frac{V_j^2(u)F_j[1 - V_{j'}(u)F_{j'}] + V_{sd}(u)V_{sf}(u)V_{df}(u)F_jF_{j'}}{[1 - V_d(u)F_d][1 - V_f(u)F_f] - V_{df}^2(u)F_dF_f}, \quad (14)$$

$$\Delta_d = \int_{-\infty}^{\infty} du P(u) \frac{V_d^2(u)F_d[1 - V_f(u)F_f] + V_{df}^2(u)F_f[1 + V_d(u)F_d]}{[1 - V_{j'}(u)F_{j'}][1 - V_f(u)F_f] - V_{df}^2(u)F_dF_f}. \quad (15)$$

Where

$$P(u) = \frac{1}{\sqrt{2\pi\beta}} e^{-u^2/2\beta}, \quad \beta = Z_{\alpha,jj'} 2T/\theta_D \quad (16)$$

is the Gauss distribution function^{23,54} and θ_D is the Debye temperature. Equation for coherent potential of the f band electrons is the same as Eq. (15) but a replacement of band indices $s \rightleftharpoons f$ is necessary.

Note also, that an assumption $|V_{n,sj}(u)F_s| \ll 1$ in Eqs. (14) and (15) means physically that the partial filling of $d(f)$ -bands sets the traps for mobile s -electrons and corresponds to the Mott idea, successfully applied previously for two band conductivity model.

On the other hand, Eq. (15) describes direct and back transitions of $d(f)$ -electrons and provides a possibility of accounting for $d(f)$ -bands modifications with temperature. These equations are solved within self-consistent loop. A solution of these equations allows one to calculate coherent potential for s -conductivity electrons.

Simple assumption leads to the previously obtained results. Indeed, using for example $V_{jj'} = 0$, i.e., neglecting the inter-band transitions, three independent equations corresponding to the single-band model of the CPA can be obtained from Eqs. (14) and (15):²³

$$\langle \Delta_j \rangle = \int_{-\infty}^{+\infty} du P(u) \frac{V_j^2(u)F_j}{1 - F_f V_j(u)}. \quad (17)$$

Also, one can found the result for two band conductivity model and perturbation theory series for the coherent potential.

Accounting for this renormalization, and also for the values of DOSes of bands and their modification with the temperature, one can estimate the magnitude of ER in actinides. Note, that effects of irradiation will not be taken into account in this result.

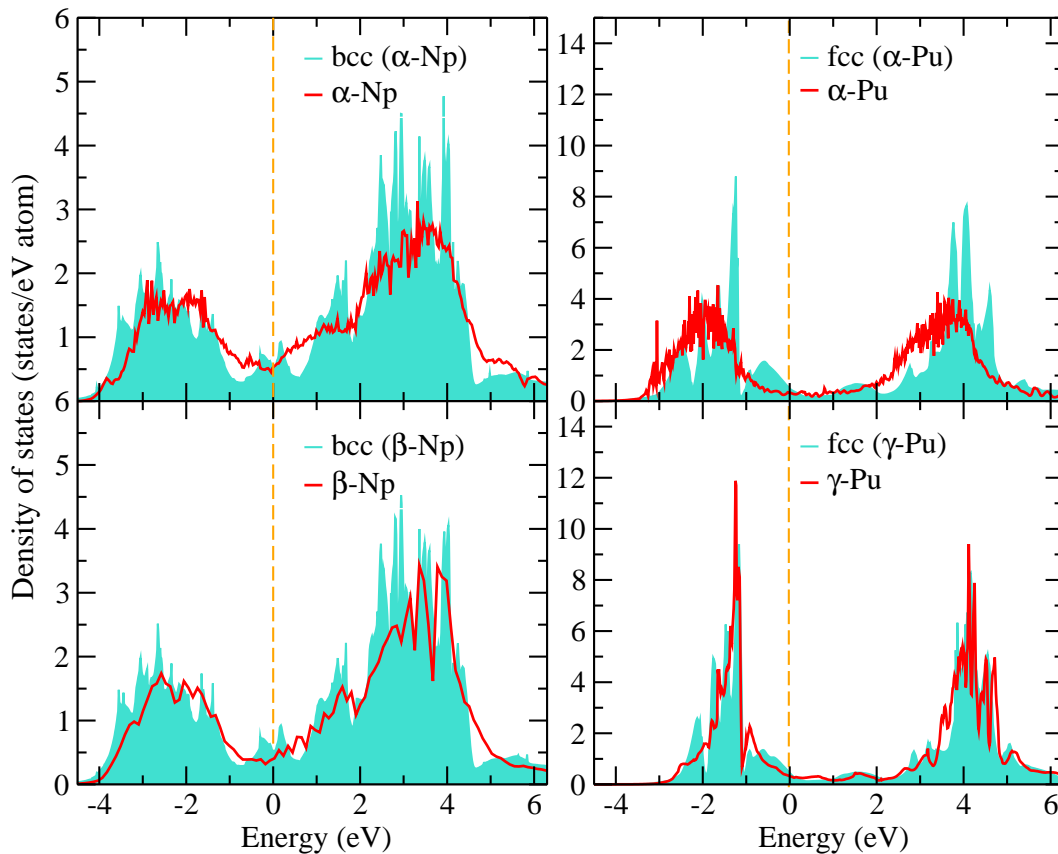


FIG. 1: (Color online) Partial 5f densities of states for α - and β -Np (left panels) and α - and γ -Pu (right panels) in real crystal structures are compared with the bcc-(Np) and fcc-(Pu) DOSes for the corresponding cell volumes per actinide atom (see Ref. 55). The Fermi energy corresponds to zero.

TABLE I: Symmetry groups of Np, Pu, Am, and Cm and results of the electronic structure calculations for the real crystal structures within the LDA+ U +SO method. The largest values of occupation matrices off-diagonal elements (OD) in $\{LS\}$ and $\{jm_j\}$ basis sets are given (see details in Ref. 33). Then the calculated values for spin (S), orbital (L), total (J) moments, Landè factor, and effective magnetic moment (μ_{eff}^{calc}) in μ_B are presented.⁵⁶

Phase	Structure	OD $_{\{LS\}}$	OD $_{\{jm_j\}}$	$n_{5/2}$	$n_{7/2}$	S	L	J	g^{calc}	μ_{eff}^{calc}, μ_B
α -Np	Pnma ⁵⁷	0.29	0.27	3.04	1.11	1.28	4.25	2.97	0.68	2.33
β -Np	P42 ₁ 2 ⁵⁸	0.33	0.31	3.12	1.20	1.33	4.46	3.13	0.68	2.44
γ -Np	Im3m ⁵⁹	0.36	0.33	3.13	1.14	1.40	4.68	3.28	0.67	2.53
α -Pu	P2 ₁ /m ⁶⁰	0.41	0.25	4.41	1.68	0	0	0	0	0
γ -Pu	C2/m ⁶⁰	0.43	0.28	4.28	1.45	0	0	0	0	0
δ -Pu	Fm3m ⁶⁰	0.45	0.01	5.57	0.24	0	0	0	0	0
AmI	P6 ₃ /mmc ⁶	0.47	0.30	4.65	1.62	0	0	0	0	0
AmII	Fm3m ⁶	0.47	0.02	5.89	0.52	0	0	0	0	0
AmIII	Fddd ⁶	0.45	0.24	3.91	2.43	0	0	0	0	0
AmIV	Pnma ⁶	0.44	0.27	4.55	1.71	0	0	0	0	0
CmI	P6 ₃ /mmc ⁵	0.33	0.51	4.71	2.88	2.85	0.91	3.76	1.76	7.44
CmII	Fm3m ⁵	0.31	0.45	4.72	2.78	2.77	0.75	3.52	1.79	7.13
CmIII	C2/c ⁵	0.31	0.49	4.82	2.82	2.77	0.75	3.52	1.79	7.13
CmIV	Fddd ⁵	0.36	0.41	4.77	2.54	2.39	0.83	3.22	1.74	6.42

IV. RESULTS

A. Ground state of metals at normal conditions and under pressure

Electronic structure of Np, Pu, Am, and Cm in real crystal structures (Table 1) were calculated within the

LDA+ U +SO method. As one can see from the analysis of off-diagonal occupation matrix elements, in all

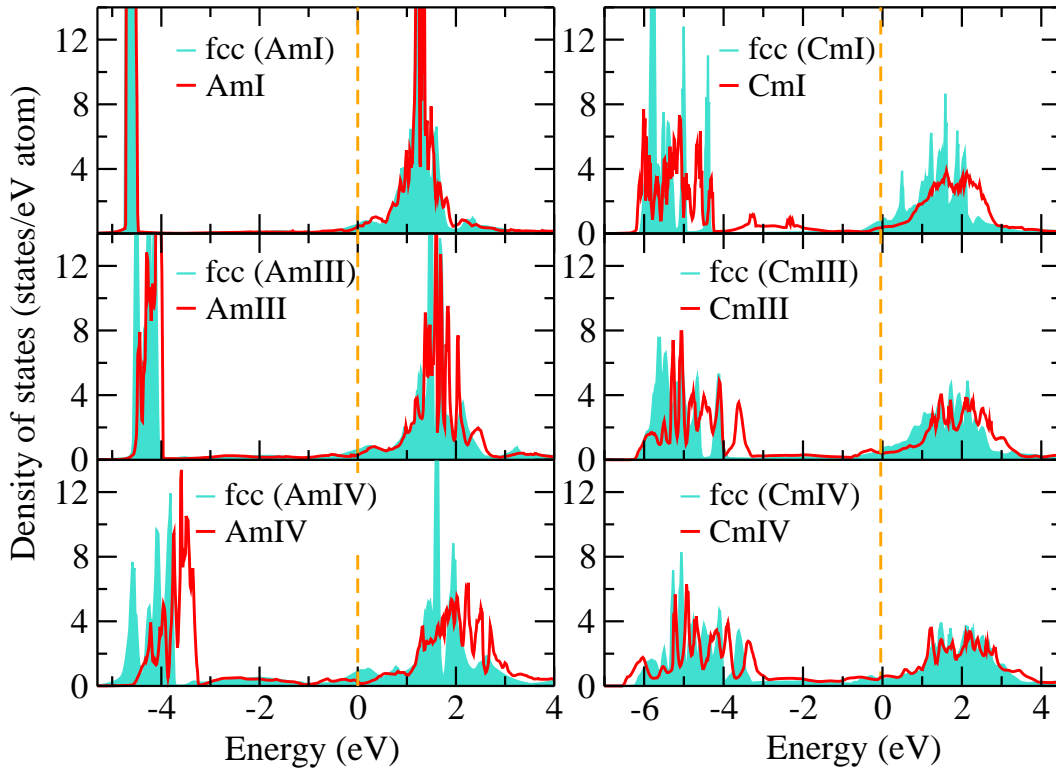


FIG. 2: (Color online) Partial $5f$ densities of states for AmI, AmIII, and AmIV (left panels) and CmI, CmIII, and CmIV (right panels) in real crystal structures are compared with the fcc-DOS for the corresponding cell volumes per actinide atom (see Ref. 55). The Fermi energy corresponds to zero.

metals (except δ -Pu and AmII) in both LS and jm_j bases off-diagonal elements are substantial and comparable. That means that intermediate coupling takes place in these metals. Simple cubic δ -Pu and AmII are well described within the jj coupling scheme that is confirmed by f^6 electronic configuration and smaller hybridization of $j = 5/2$ subband with $j = 7/2$ subband and reflected in its smaller occupation.

In all our calculations for Pu and Am only nonmagnetic solution was found, whereas in neptunium effective magnetic moment was obtained about $3 \mu_B$ and depends on phase. In curium effective magnetic moment strongly differs in the phases, see Table 1. Experimental value of the moment in Cm was measured as $7.85 \mu_B$.⁶¹ While model calculations predict magnetic moment from $7.94 \mu_B$ in ionic picture in the assumption of pure LS coupling to $7.6 \mu_B$ in the assumption of intermediate coupling.⁶¹

For the many-band conductivity model presented in Section III partial densities of states from *ab initio* calculations are used. In Figs. 1 and 2 we present $5f$ partial densities of states for the calculated crystal phases. Results for cubic (γ -Np, δ -Pu, AmII, and CmII) structures under pressure were reported elsewhere.⁵⁵ In all DOSes one can distinguish two groups of peaks attributed to the subbands with the total moment value $j = 5/2$ at the lower energies and $j = 7/2$ at higher ones splitted

by strong spin-orbit coupling. The Fermi level is shifted upward from the upper slope of $j = 5/2$ subband in Pu and crosses the $j = 7/2$ subband in Cm corresponding to the increasing number of f electrons. A separation of the centers of gravity of these subbands for the value of Coulomb parameter $U = 4$ eV results in $5 - 5.5$ eV.

For comparison we present DOSes of the cubic phase under pressure calculated within LDA+ U +SO for the corresponding volumes per actinide atom. As one can see, cubic phases with the fitted volumes can be used as a good approximation for real phases $5f$ DOSes, since the centers of gravity and bandwidth of $j = 5/2$ and $7/2$ subbands are found in good agreement with that in the real phases. Also the total density of states of real and corresponding cubic phases at the Fermi level are close. Having this close similarity in mind, below we report the resistivity model results for the DOSes of cubic phases with different volumes taken as a starting point. Since the model allows to estimate temperature dependence of ER, the starting DOSes were temperature broadened. The result of such broadening for curium in the volumes per atom, corresponding to real volumes are shown in Fig. 3. All other DOSes before broadening are reported in Ref. 55 and look similar with the broadening.

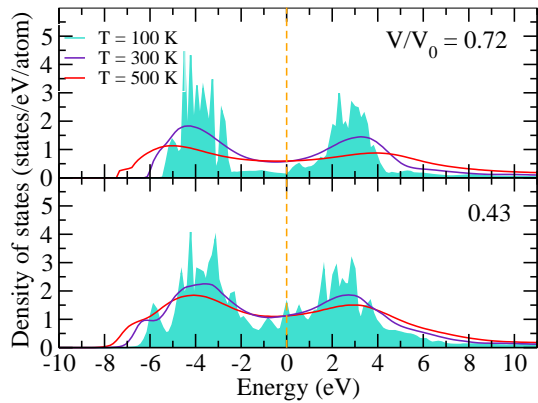


FIG. 3: (Color online) Partial 5f densities of states of some fcc-curium volumes under pressure the CPA broadened for the temperatures $T = 100, 300,$ and 500 K. Here the volumes are related to V_0 – the volume per ion in CmI phase at ambient pressure. The Fermi energy corresponds to zero.

B. Electrical resistivity temperature dependencies of metals at normal conditions and under pressure

Electrical resistivity in CPA is usually calculated within Kubo formula for the diagonal part of conductivity tensor

$$\sigma = (\rho)^{-1} = \sum_j \frac{4e^2 \hbar n_j}{3\pi^2 m^*} \int dU \left(-\frac{df}{dU}\right) \times \Upsilon(U) \quad (18)$$

where

$$\Upsilon(U) = \int dE g_j(E) E \left[\frac{\gamma_j(U)}{(U - E - \eta_j(U))^2 + \gamma_j^2(U)} \right]^2, \quad (19)$$

and g_j is DOS of the j -th conductivity band. In this equation, the approximate expression $v^2 = 2E/m^*$ for the square of electron velocity was used. Note, that apparent limitations of Eq. (18) arise from neglecting of back $f(d) \rightarrow s$ transitions of conductivity electrons.²³

Numerical solution of Eqs. (14) and (15) with $s, d,$ and f DOSes of metal provides a usual way to estimate effective mass of conductivity electrons (m_j^*) from *ab initio* results. Accounting for effective mass renormalization and “accepting” DOSes modification with temperature, one can try to estimate the absolute values of ER of actinides. However, this result will comprise no correction on effects of irradiation.

Full solution of the CPA Eq. (15) for pure fcc-Pu, Am, Cm and bcc-Np metals at normal conditions and under pressure were obtained using corresponding *ab initio* DOSes⁵⁵ as the starting point of iteration procedure. Bloch constant value equal to $0.8 E_F$ ³⁰ and experimental data for the Debye temperature^{30,32} $\theta_D \sim 100K$, velocity of sound and structural data (see Table 1) were used for the parametrization of these equations. Note, that

the Debye temperature estimations^{30,32,62} presented previously for δ -Pu by other authors differ significantly from each other. However, simulations within self-consistent general thermodynamic model, accounting for effect of anharmonicity of lattice⁶³ gives the same value for Debye temperature as found experimentally in Ref. 30.

It is well known that the value of DOS and its behavior in the vicinity of the Fermi level affect significantly kinetic properties of metal. All DOSes modifications with temperature and pressure has attracted a great deal of attention. The present results are based on the common numerical solution of a set of CPA equations (15), performed for different pressure and temperature and demonstrate general trend of strong influence of electron phonon interaction on the initial DOS. In Fig. 3 the densities of states for a few volumes of curium are shown to illustrate the temperature broadening of DOSes. One can see from Fig. 3, that strong electron-phonon coupling leads to significant smoothing of all initial fine features of the DOS curves. At the same time, applied pressure is slightly hindered the smoothing of the initial curve but does not lead to qualitatively different result. In vicinity of the melting point, calculated DOSes of all metals completely lose all their original features and are similar to each other. Calculated dynamics of DOSes evolution determines mainly the behavior of ER vs. temperature and applied pressure.

Recently, ER calculations for pure bcc-Np, fcc-Pu, Am, and Cm metals within CPA for two band conductivity model at high temperatures and normal conditions proposed typical metallic behavior of ER over the whole temperature region without any specific peculiarities.²³ Similar behavior of ER vs. temperature without any anomalies and singularities were calculated in this work for actinides within the proposed conductivity model both at normal conditions and under pressure. For bcc-Np and fcc-Cm metal only the phonon part of ER was calculated. For pure fcc-Pu and Am at high temperature ER is defined by electron-phonon scattering mainly.

One can see, that all theoretical curves of ER are similar to the common curves measured for a number of $4d$ -($5d$ -) transition metals⁶⁴ and agree well with the experimental data. Calculated dependencies of ER for all metals show, that the TCR of the metals increases with the pressure and decrease with temperature for $100 \div 500$ K. In the vicinity of melting point TCR for all metals was found to be a weakly increasing function of temperature.

Np metal. The first detailed ER experimental data on temperature dependence of pure orthorhombic α -Np phase with $R_{295}/R_{4.2} = 34.36$ was reported in 1963.¹⁹ Subsequent experiments (see Ref. 15) were performed for polycrystalline samples of α -Np in $4.2 - 300$ K temperature range. The residual resistivity of the Np metal was found to be equal to $12.2 \mu\Omega cm$ and $R_{273}/R_{4.2} = 8.15$,¹⁵ that shows high concentration of different impurities in the samples. Authors of Ref. 20 reported Np $R_{273}/R_{4.2}$ value to be equal to 4.47 and pointed out strong effect of self-damage on the observed value of ER.

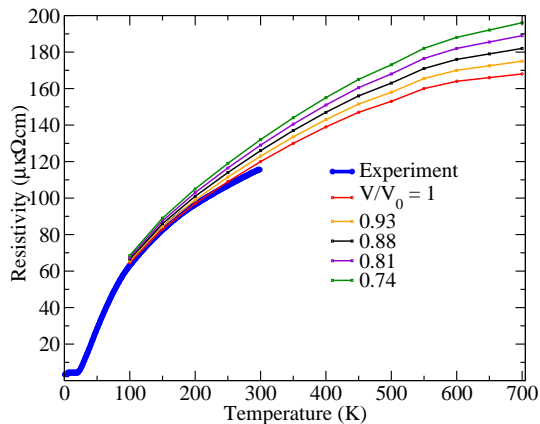


FIG. 4: (Color online) Electrical resistivity of Np metal under pressure. For each curve the corresponding volume is related to the volume per actinide ion (V_0) at ambient pressure – V/V_0 .

Note, that residual resistivity values about $10 \div 15 \mu\Omega cm$ are typical in concentrated $3d$ - and $5d$ -transition metal alloys with strong electron impurity interaction. After subtraction of this background the temperature dependence of ER of Np was found to be ordinary for *dilute alloys* with $\rho \sim T^3$ in low temperature region⁶⁵ and a weakly increasing non-linear function of temperature $T > \theta_D$. The calculated ER values agree well with experimental data in arbitrary units at normal conditions and predicts TCR increasing under pressure. Calculations of conductivity of $s(p)$ -, d -, and f -electrons show that total ER is determined by $s(p)$ -electrons mainly and partially by d -electrons. Assuming that f -band electrons are conducting ones, we obtained strongly overestimated ER values. Determining the temperature-dependent part of ER as $\rho(T) - \rho_0$ and using calculated values of ER of s - and d -electrons, we found the resistivity values underestimated by 9–11 %. That is why only electron-phonon interaction was taken into consideration and electron-electron coupling was neglected.

Pu metal. Negative TCR value in α -Pu were measured about five decades ago.¹⁴ This result is unique for pure metal and was confirmed by several groups.^{16,17} Experimental results for ER motivated great discussion of possible mechanism of scattering which can provide such values of negative coefficient of resistivity and a model explaining it.

However, note at first that α -Pu as well as δ -Pu have very high values of residual resistivity and high concentrations of impurities and defects. Strong change of ER values during the holding time also evidences for strong contributions of electron-impurity and electron-defect scattering parts to the total value of resistivity. Second, thus experimental data were obtained for dilute Pu-based alloys and quasi-polycrystalline samples.

Using well-known experimental fact that ER of poly-

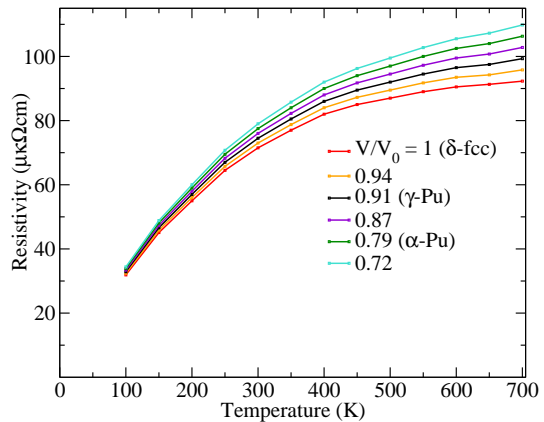


FIG. 5: (Color online) Electrical resistivity of Pu metal under pressure.

crystalline metals shows behavior analogous to their fcc- and bcc-crystal phases, the negative TCR can easily be explained in terms of electrons scattering on non-coherent phonons. Indeed, electron scattering on lattice defects, produced by self-damage in α -Pu and ion mass modification as a result of irradiation leads to randomly distributed “impurity” ions on the sites of crystal lattice. Hence, conductivity electrons scatter not only on “pure” phonons but also on randomly distributed Coulomb fields of impurities ions. This model equivalence corresponds to interference model of scattering in fcc- dilute Pu-based alloys (δ -Pu), previously proposed and discussed in Refs. 23 and 31. This consideration can be extended, allowing a direct way to explain complex experimental data as well as non-magnetic nature of the observed ER anomalies, $\rho \sim T^2$ at low temperature, negative TCR at high temperature range and exclude α -Pu from list of anomalous metals, at least concerning its resistivity properties.

Electrical resistivity calculations of fcc-Pu within proposed *many-band* conductivity model were performed in absolute units. Experimental ER data for pure fcc-Pu are unknown. Numerical simulation shows ordinary temperature dependence of ER at high temperature. An attempt to separate resistivity of different groups of electrons gives domination of s -band electrons with effective mass above $25 \div 30$ at high pressure and $\sim 35 \div 40$ at normal condition. The electron mass renormalization is the result of intensive $s \rightarrow d$ and $s \rightarrow f$ transitions and strong effect of direct $d \rightarrow f$ and back $f \rightarrow d$ transitions on the DOS values at the Fermi level. Calculated absolute values of ER underestimate experimental data for α -Pu and δ -Pu by a factor of 3 and predict metallic type of temperature dependencies of resistivity at normal conditions and under pressure. TCR of Pu was calculated as a weak increasing function of pressure and weak decreasing function of temperature.

Am metal. During the last five years high interest in resistance properties of Am arose due to superconductivity found in pure metal. Reported values of T_c of Am

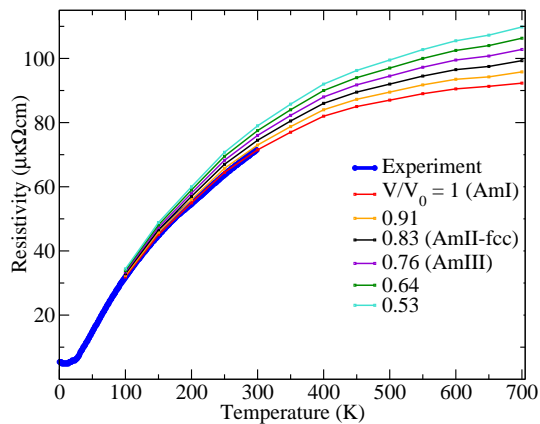


FIG. 6: (Color online) Electrical resistivity of Am metal under pressure.

metal is above 0.5 K and found to be dependent on applied pressure.²²

Electrical resistivity of pure Am metal was reported for the first time in Ref. 18. The samples were relatively pure and low temperature behavior of Am metal was obtained as $\rho(T) \sim T^{4 \pm 0.5}$, that agrees well with the data for transition metals containing small number of impurities. At high temperature ER demonstrates also ordinary dependence with decreasing TCR for all investigated temperatures.

Calculations performed within the proposed model at normal conditions and pressure show ordinary ER temperature dependencies and agree well with experiments, see Fig. 6. Obtained TCR is a decreasing function of temperature in all regions but slightly increasing with applied pressure. Numerical values of ER underestimate experimental data by 10 – 15 %. Nature of the obtained ER dependencies is analogous to calculated for Np and Pu ones and determined mainly by renormalization of DOSes with temperature.

At this time nothing can be say about giant values – $\sim 400 \mu k\Omega cm$ of ER of Am-IV, obtained at room temperature and ambient pressure 25-30 GPa.²² Moreover, these giant values of ER were measured in the system with typical metal type of conductivity without any sign of metal-semiconductor transition. All possible model’s assumptions, accounting for different scattering mechanisms of conductivity of electrons and very optimistic expectations give ER values about 150-200 $\mu k\Omega cm$ only. The nature of high resistivity state can be explained assuming for example, that heavy electrons of *d*- and *f*-bands are the conductivity electrons and *s*-type electrons are excluded from charge transport process. However, we have no corresponding experimental data to point out this opinion.

Cm metal. Only recently experimental data on ER in α -Cm (Cm-I) were reported. Total ER was found as a sum of residual resistivity (more than 40 $\mu k\Omega \cdot cm$), magnetic part of resistivity, and the part of ER origi-

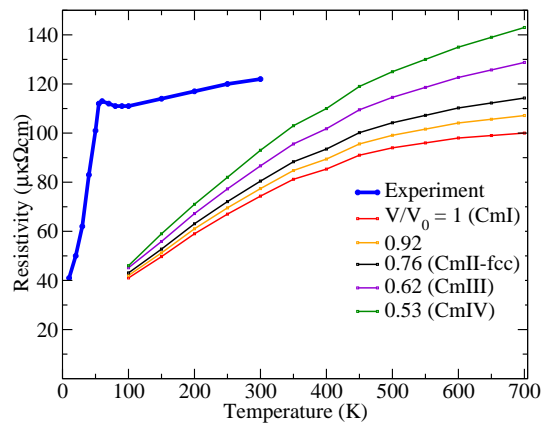


FIG. 7: (Color online) Electrical resistivity of Cm metal under pressure.

nated from electron-phonon coupling.⁶⁶ ER behavior of Cm is typical for antiferromagnetic metal and transparent anomalies in the vicinity of the Neel point. The magnetic part of ER was determined as a difference between the total resistivities of Cm and Am. Note first, that the large value of residual resistivity shows that the investigated samples of Cm metal contained a substantial number of impurities, including non-controlled ones. Second, nothing can be said about reliability of the suggestion, proposed in Ref. 66, that total ER is a sum of additive values, since strong electron-impurity interaction can significantly correct this result.

In the present paper only the “phonon” part of the total ER in Cm was determined and discussed unambiguously. The calculated ER is a usual linear function of temperature with positive TCR in the interval of 100 – 350 K and has similar behavior as in Pu and Am at the higher temperature. Temperature coefficient of resistivity of Cm demonstrates small decreasing under pressure, the similar one was calculated for the other metals under consideration. For this reason in Cm the DOS value at the Fermi level does not change drastically with temperature and mainly the T/Θ factor determines the temperature behavior of ER. Note, that from 500 to 700 K the ER of metals has weak temperature dependence and reaches its high temperature limit due to strong erosion of DOS at the Fermi level.

V. CONCLUSION

We report the results of model calculations of electrical resistivity for Np, Pu, Am, and Cm metals under pressure within CPA for many-bands conductivity model. We used DOSes of the metals under consideration as a starting point in our model calculations. For this purpose, Np, Pu, Am, and Cm pure metals were investigated in real crystal phases within the LDA+*U* method with spin-orbit coupling (LDA+*U*+SO). For Am and Pu metals in

all structures we found nonmagnetic ground state. We compared DOSes calculated for the real crystal structures of the transuranium metals with the DOSes for corresponding fcc volumes per actinide atom. It follows from this comparison that total density of states, as well as centers of gravity and bandwidth of $j = 5/2$ and $7/2$ subbands are in good agreement. It means that the cubic structures in different volumes provide good estimation for the DOSes of real crystal structures.

Results of our CPA calculations within derived many-band conductivity model for *pure* fcc-Pu, Am, and Cm and bcc-Np using Bloch constant value $\sim 0.8E_F$ ³⁰ and *ab initio* DOSes of metals show ordinary metal type of ER behavior vs. temperature at normal conditions and under pressure. High values of ER in these metals are a consequence of $s \rightarrow d$ and $s \rightarrow f$ transitions of scattering electrons and effective mass of conductivity electrons increasing as a result of s - and d -electron bands hybridization. Weak non-linearity in the ER temperature behavior of metals above θ_D is caused by DOS erosion at the Fermi level due to electron-phonon interaction.

The obtained high-resistivity values in actinides result from $s \rightarrow d$ and $s \rightarrow f$ interband transitions and conductivity electron mass renormalization due to strong s - d hybridization. Also strong influence on the ER temperature dependencies of actinides is a result of DOS of accepting bands modifications as products of direct $s \rightarrow d$ and

$d \rightarrow f$ and back $f \rightarrow d$ electrons transitions. Calculated phonon part of resistivity underestimates experimental data by a factor of 1.5 for Cm and by a factor of 3 for ideal Pu.

VI. ACKNOWLEDGMENTS

The authors are grateful to M. Fluss and L. Timofeeva for stimulating conversations. This work was supported by the Russian Foundation for Basic Research, projects nos. 10-02-00046a, 09-02-00431a, and 10-02-00546a, Russian Federal Agency for Science and Innovations (Program ‘‘Scientific and Scientific-Pedagogical Training of the Innovating Russia’’ for 2009-2010 years), grant No. 02.740.11.0217, the Scientific program ‘‘Development of scientific potential of universities’’ no. 2.1.1/779.

VII. APPENDIX

Let us assume that the matrix elements of interaction $V_{ll'}$ are averaged over the angle between the wave vectors \vec{k} and \vec{k}' and thus depend only on the band index. Using this simplification and Eq. (13), one obtains:

$$\hat{\Delta} = \frac{1}{N} \sum_{ln} e^{i(\vec{k}-\vec{k}', \vec{R}_n)} \left\{ \sum_{j_1} [V_{jj_1}(u)] F_{j_1} [V_{j_1 j'}(u)] + \sum_{j_1 j_2} [V_{jj_1}(u)] F_{j_1} [V_{j_1 j_2}(u)] F_{j_2} [V_{j_2 j'}(u)] + \dots \right\} \delta_{ll'} a_l^\dagger a_{l'}, \quad (20)$$

where the j -th band electron Green function F_j is defined as

$$F_j = \frac{1}{N} \sum_{\vec{k}} \frac{1}{(z - E_{\vec{k},j} - \Delta_j)}. \quad (21)$$

Comparing Eqs. (8) and (20), for Δ_j one obtains

$$\Delta_{j'} = \sum_{j_1} [V_{jj_1}(u)] F_{j_1} [V_{j_1 j'}(u)] + \sum_{j_1 j_2} [V_{jj_1}(u)] F_{j_1} [V_{j_1 j_2}(u)] F_{j_2} [V_{j_2 j'}(u)] + \dots \quad (22)$$

Using the following matrix form

$$[F] = \begin{bmatrix} F_s & 0 & 0 \\ 0 & F_d & 0 \\ 0 & 0 & F_f \end{bmatrix}, \quad [\Delta] = \begin{bmatrix} \Delta_s & 0 & 0 \\ 0 & \Delta_d & 0 \\ 0 & 0 & \Delta_f \end{bmatrix}, \quad [V] = \begin{bmatrix} V_{n,ss}(u) & V_{n,sd}(u) & V_{n,sf}(u) \\ V_{n,ds}(u) & V_{n,dd}(u) & V_{n,df}(u) \\ V_{n,fs}(u) & V_{n,fd}(u) & V_{n,ff}(u) \end{bmatrix}, \quad (23)$$

the series (13) is summed up accurately in the convergence range $|V_j(u)F_j| < 1$. Within single-electron and single-site approaches that gives

$$\langle [\Delta] \rangle = \langle [V][F][V] + [V][F][V][F][V] + \dots \rangle = \left\langle \frac{[V][F][V]}{1 - [F][V]} \right\rangle. \quad (24)$$

Calculating matrix products and averaging over phonons both part of Eq. (24), the set of CPA equations can be obtained.

- * Electronic address: y.tsiovkin@mail.ustu.ru
- ¹ *Challenges in Plutonium Science*, edited by N. G. Cooper, Los Alamos Sci. **26** (LANL, Los Alamos, NM, 2000).
 - ² D. A. Young, *Phase diagram of the Elements* (University of California Press, Berkeley, 1991).
 - ³ S. S. Hecker, D. R. Harbur, and T. G. Zocco, *Prog. Mater. Sci.* **49**, 429 (2004).
 - ⁴ G. H. Lander, *Science* **301**, 1057 (2003).
 - ⁵ S. Heathman, R. G. Haire, T. Le Bihan, A. Lindbaum, M. Idiri, P. Normile, S. Li, R. Ahuja, B. Johansson, and G. H. Lander, *Science* **309**, 110 (2005).
 - ⁶ S. Heathman, R. G. Haire, T. Le Bihan, A. Lindbaum, K. Litfin, Y. Mèresse, and H. Libotte, *Phys. Rev. Lett.* **85**, 2961 (2000).
 - ⁷ A. Lindbaum, S. Heathman, K. Litfin, Y. Mèresse, R. G. Haire, T. Le Bihan, and H. Libotte, *Phys. Rev. B* **63**, 214101 (2001).
 - ⁸ G. van der Laan, K. T. Moore, J. G. Tobin, B. W. Chung, M. A. Wall, and A. J. Schwartz, *Phys. Rev. Lett.* **93**, 097401 (2004); G. van der Laan and B. T. Thole, *Phys. Rev. B* **53**, 14 458 (1996).
 - ⁹ K. T. Moore, M. A. Wall, A. J. Schwartz, B. W. Chung, D. K. Shuh, R. K. Schulze, and J. G. Tobin, *Phys. Rev. Lett.* **90**, 196404 (2003); K. T. Moore, M. A. Wall, A. J. Schwartz, B. W. Chung, S. A. Morton, J. G. Tobin, S. Lazar, F. D. Tichelaar, H. W. Zandbergen, P. Söderlind, and G. van der Laan, *Philos. Mag.* **84**, 1039 (2004).
 - ¹⁰ K. T. Moore and G. van der Laan, *Rev. Mod. Phys.* **81**, 235 (2009).
 - ¹¹ K. T. Moore, G. van der Laan, R. G. Haire, M. A. Wall, A. J. Schwartz, and P. Söderlind, *Phys. Rev. Lett.* **98**, 236402 (2007).
 - ¹² H. Ledbetter, A. Lawson, and A. Migliori, *J. Phys.: Condens. Matter* **22**, 165401 (2010).
 - ¹³ A. M. Boring and J. L. Smith, *Los Alamos Sci.* **26**, 90 (2000); S. S. Hecker and J. C. Martz, *ibid.* **26**, 238 (2000).
 - ¹⁴ R. Smoluchowski, *Phys. Rev.* **125**, A1577 (1962).
 - ¹⁵ C. E. Olsen and R. O. Elliott, *Phys. Rev.* **139**, A437 (1965).
 - ¹⁶ M. B. Brodsky, *Phys. Rev.* **137**, A1423 (1965).
 - ¹⁷ M. B. Brodsky, *Rep. Prog. Phys.* **41**, 1547 (1978).
 - ¹⁸ W. Müller, R. Schenkel, H. E. Schmidt, J. C. Spirlet, D. L. McElroy, R. O. A. Hall, and M. J. Mortimer, *J. Low Temp. Phys.* **30**, 561 (1978).
 - ¹⁹ G. T. Meaden, *Proc. R. Soc. Lond. A* **276**, 553 (1963).
 - ²⁰ E. King, J. A. Lee, K. Mendelsohn, and D. A. Wigley, *Proc. R. Soc. Lond. A* **284**, 325 (1965).
 - ²¹ It is a well-known fact, that the order in $\rho \sim T^n$ dependencies increases up to $n = 5$ with purity of transition metals.
 - ²² J.-C. Griveau, J. Rebizant, G. H. Lander, and G. Kotliar, *Phys. Rev. Lett.* **94**, 097002 (2005).
 - ²³ Yu. Yu. Tsiovkin, M. A. Korotin, A. O. Shorikov, V. I. Anisimov, A. N. Voloshinskii, A. V. Lukoyanov, E. S. Koneva, A. A. Povzner, and M. A. Surin, *Phys. Rev. B* **76**, 075119 (2007).
 - ²⁴ S. Méot-Reymond and J. M. Fournier, *J. Alloys Compd.* **232**, 119 (1996).
 - ²⁵ V. Dallacasa, *J. Phys.: F Metal Phys.* **11**, 177 (1981).
 - ²⁶ M. Fluss, B. D. Wirth, M. Wall, T. E. Felter, M. J. Caturla, A. Kubota, and T. Diaz de la Rubia, *J. Alloys Compd.* **368**, 62 (2004).
 - ²⁷ R. Jullien, M. T. Beal-Monod, and B. Cogblin, *Phys. Rev. B* **4**, 1441 (1974).
 - ²⁸ Yu. Piskunov, K. Mikhalev, A. Gerashenko, A. Pogudin, V. Ogloblichev, S. Verkhovskii, A. Tankeyev, V. Arkhipov, Yu. Zouev, and S. Lekomtsev, *Phys. Rev. B* **71**, 174410 (2005).
 - ²⁹ S. V. Verkhovskii, V. E. Arkhipov, Yu. N. Zuev, Yu. V. Piskunov, K. N. Mikhalev, A. V. Korolev, I. L. Svyatov, A. V. Pogudin, V. V. Ogloblichev, and A. L. Bulzlov, *JETP Lett.* **82**, 139 (2005).
 - ³⁰ J. C. Lashley, J. Singleton, A. Migliori, J. B. Betts, R. A. Fisher, J. L. Smith, and R. J. McQueeney, *Phys. Rev. Lett.* **91**, 205901 (2003).
 - ³¹ Yu. Yu. Tsiovkin and L. Yu. Tsiovkina, *J. Phys.: Condens. Matter* **19**, 056207 (2007).
 - ³² J. C. Lashley, A. C. Lawson, R. J. McQueeney, and G. H. Lander, *Phys. Rev. B* **72**, 054416 (2005).
 - ³³ A. O. Shorikov, A. V. Lukoyanov, M. A. Korotin, and V. I. Anisimov, *Phys. Rev. B* **72**, 024458 (2005).
 - ³⁴ A. B. Shick, V. Drchal, and L. Havela, *Europhys. Lett.* **69**, 588 (2005).
 - ³⁵ A. B. Shick, J. Kolorenč, A. I. Lichtenstein, and L. Havela, *Phys. Rev. B* **80**, 085106 (2009).
 - ³⁶ L. Havela, A. Shick, and T. Gouder, *J. Appl. Phys.* **105**, 07E130 (2009).
 - ³⁷ R. Atta-Fynn and A. K. Ray, *Europhys. Lett.* **85**, 27008 (2009).
 - ³⁸ F. Cricchio, F. Bultmark, and L. Nordström, *Phys. Rev. B* **78**, 100404 (2008).
 - ³⁹ F. Bultmark, F. Cricchio, O. Granäs, and L. Nordström, *Phys. Rev. B* **80**, 035121 (2009).
 - ⁴⁰ G. Kotliar, S. Y. Savrasov, K. Haule, V. S. Oudovenko, O. Parcollet, and C. A. Marianetti, *Rev. Mod. Phys.* **78**, 865 (2006).
 - ⁴¹ S. Y. Savrasov, G. Kotliar, and E. Abrahams, *Nature (London)* **410**, 793 (2001).
 - ⁴² L. V. Pourovskii, M. I. Katsnelson, A. I. Lichtenstein, L. Havela, T. Gouder, F. Wastin, A. B. Shick, V. Drchal, and G. H. Lander, *Europhys. Lett.* **74**, 479 (2006).
 - ⁴³ L. V. Pourovskii, G. Kotliar, M. I. Katsnelson, and A. I. Lichtenstein, *Phys. Rev. B* **75**, 235107 (2007).
 - ⁴⁴ J. H. Shim, K. Haule, and G. Kotliar, *Nature (London)* **446**, 513 (2007).
 - ⁴⁵ J. H. Shim, K. Haule, and G. Kotliar, *Europhys. Lett.* **85**, 17007 (2009).
 - ⁴⁶ J.-X. Zhu, A. K. McMahan, M. D. Jones, T. Durakiewicz, J. J. Joyce, J. M. Wills, and R. C. Albers, *Phys. Rev. B* **76**, 245118 (2007).
 - ⁴⁷ C. A. Marianetti, K. Haule, G. Kotliar, and M. J. Fluss, *Phys. Rev. Lett.* **101**, 056403 (2008).
 - ⁴⁸ J. G. Tobin, P. Söderlind, A. Landa, K. T. Moore, A. J. Schwartz, B. W. Chung, M. A. Wall, J. M. Wills, R. G. Haire, and A. L. Kutepov, *J. Phys.: Condens. Matter* **20**, 125204 (2008).
 - ⁴⁹ V. I. Anisimov, F. Aryasetiawan, and A. I. Lichtenstein, *J. Phys.: Condens. Matter* **9**, 767 (1997).
 - ⁵⁰ V. I. Anisimov and O. Gunnarsson, *Phys. Rev. B* **43**, 7570 (1991).
 - ⁵¹ O. Gunnarsson, O. K. Andersen, O. Jepsen, and J. Zaanen, *Phys. Rev. B* **39**, 1708 (1989).
 - ⁵² All calculations were performed in the TB-LMTO-ASA

- package. O. K. Andersen, Phys. Rev. B **12**, 3060 (1975).
- ⁵³ A. N. Voloshinskii and A. G. Obukhov, Phys. Met. Metallogr. **91**, 238 (2001).
- ⁵⁴ A. B. Chen, G. Weisz, and A. Sher, Phys. Rev. B **5**, 2897 (1972).
- ⁵⁵ A. V. Lukoyanov, A. O. Shorikov, V. B. Bystrushkin, A. A. Dyachenko, L. R. Kabirova, Yu. Yu. Tsiovkin, A. A. Povzner, V. V. Dremov, M. A. Korotin, and V. I. Anisimov, arXiv:1005.2851.
- ⁵⁶ For the phases with several inequivalent actinide ions we found close values of the off-diagonal elements and moments. For such phases the averaged values per ion and the largest OD elements are given.
- ⁵⁷ W. H. Zachariasen, Acta Crystallogr. **5**, 660 (1952).
- ⁵⁸ W. H. Zachariasen, Acta Crystallogr. **5**, 664 (1952).
- ⁵⁹ W. B. Pearson, *Handbook of Lattice Spacings and Structures of Metals and Alloys*, (Pergamon, New York, 1967), Vol. 2.
- ⁶⁰ W. H. Zachariasen and F. H. Ellinger, Acta Crystallogr. **8**, 431 (1955); *ibid.* **16**, 777 (1963).
- ⁶¹ P. G. Huray and S. E. Nave, in *Handbooks on the Physics and Chemistry of the Actinides*, edited by A. J. Freeman and G. H. Lander (Elsevier, Amsterdam, 1985), Vol. 5, p. 311.
- ⁶² H. Ledbetter, A. Migliori, J. Betts, S. Harrington, and S. El-Khatib, Phys. Rev. B **71**, 172101 (2005).
- ⁶³ A. N. Filanovich, A. A. Povzner, V. Yu. Bodryakov, Yu. Yu. Tsiovkin, and V. V. Dremov, Technical Physics Letters **35**, 929 (2009).
- ⁶⁴ T. Aisaka and M. J. Shimizu, J. Phys. Soc. Jap. **28**, 646 (1970).
- ⁶⁵ The dependence $T^{3.12}$ is more correct.¹⁹
- ⁶⁶ R. Schencel, Solid State Comm. **23**, 389 (1977).